Acta Crystallographica Section F
Structural Biology Communications
ISSN 2053-230X

Crystallization and structure determination of a symmetrical 'football' complex of the mammalian mitochondrial Hsp60–Hsp10 chaperonins

Shahar Nisemblat,[a,b] Avital Parnas,[a,b] Oren Yaniv,[b,c] Abdussalam Azem[a,b]* and Felix Frolow[b,c]*

[a]Department of Biochemistry and Molecular Biology, George S. Wise Faculty of Life Sciences, Tel Aviv University, 69978 Tel Aviv, Israel, [b]The Daniella Rich Institute for Structural Biology, George S. Wise Faculty of Life Sciences, Tel Aviv University, 69978 Tel Aviv, Israel, and [c]Department of Molecular Microbiology and Biotechnology, George S. Wise Faculty of Life Sciences, Tel Aviv University, 69978 Tel Aviv, Israel

Correspondence e-mail: azema@tauex.tau.ac.il, mbfrolow@post.tau.ac.il

Received 23 October 2013
Accepted 15 December 2013

The mitochondrial Hsp60–Hsp10 complex assists the folding of various proteins impelled by ATP hydrolysis, similar to the bacterial chaperonins GroEL and GroES. The near-atomic structural details of the mitochondrial chaperonins are not known, despite the fact that almost two decades have passed since the structures of the bacterial chaperonins became available. Here, the crystallization procedure, diffraction experiments and structure determination by molecular replacement of the mammalian mitochondrial chaperonin HSP60 (E321K mutant) and its co-chaperonin Hsp10 are reported.

1. Introduction

Mammalian cells contain two types of 60 kDa chaperonin proteins, one residing in the cytosol and the other within the mitochondrial matrix. The latter protein belongs to the type I chaperonin family that is also found in eubacteria and chloroplasts. The proteins of this family play a vital role in mediating the folding of newly translated, imported or stress-denatured proteins in an ATP-dependent manner (Cheng *et al.*, 1989; Levy-Rimler *et al.*, 2002; Bross *et al.*, 2012).

Owing to the ready availability and the marked stability of the bacterial chaperonin system, most of our understanding of chaperonin structure and function comes from investigation of the GroE chaperonin proteins (GroEL and GroES) from *Escherichia coli*. The crystal structure of GroEL was solved almost two decades ago, revealing a molecule comprised of 14 60 kDa subunits that are organized in two heptameric rings stacked back to back (PDB entries 1grl and 1aon; Braig *et al.*, 1994; Xu *et al.*, 1997). The internal hollow parts of the rings create a central cavity also known as the 'Anfinsen cage' (Ellis, 2003). Elucidation of the co-chaperonin structure of GroES in the bacterial GroEL–GroES complex showed that it forms a dome-shaped ring consisting of seven identical 10 kDa subunits (Hunt *et al.*, 1996). It serves as a 'cap' for the Anfinsen cage, allowing the formation of an isolated niche in which the substrate can fold in an ATP-dependent manner (Xu *et al.*, 1997).

The mitochondrial chaperonins Hsp60 and Hsp10 (mHsp60 and mHsp10) play crucial roles in the folding of newly imported matrix proteins (Ostermann *et al.*, 1989; Cheng *et al.*, 1989). Numerous previous studies have revealed that there are some significant differences between the bacterial and the mitochondrial chaperonins with respect to their oligomeric state, the effect of nucleotides on their interaction with co-chaperonins and their ability to function with co-chaperonins from different sources (Parnas *et al.*, 2012; Nielsen & Cowan, 1998; Nielsen *et al.*, 1999; Viitanen *et al.*, 1992). Moreover, it has been shown (Cappello *et al.*, 2008; Deocaris *et al.*, 2006; Samali *et al.*, 1999; Gupta & Knowlton, 2005; Osterloh *et al.*, 2004; Czarnecka *et al.*, 2006) that mHsp60 also plays key roles outside mitochondria. Altogether, these findings suggest that the mechanism of action of the mammalian mitochondrial chaperonins is distinct from those of the bacterial system. The structural basis underlying the extracellular functions of mHsp60 is still unknown and no high-resolution information is yet available for mHsp60 or its interacting co-chaperonin mHsp10.

To gain insight into the unique properties of mHsp60, we set out to crystallize this protein in complex with its co-chaperonin. Because of

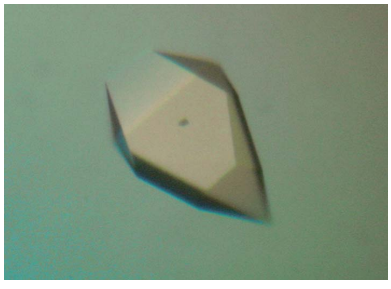

the labile nature of mHsp60 and of its complex with mHsp10, we used the previously described mutant mHsp60^{E321K} (Parnas *et al.*, 2012). This mutant has been shown to stabilize the open conformation of mHsp60 and to create a very stable complex between mHsp60 and mHsp10. Use of this mutant is expected to stabilize the R′R′ allosteric state of the protein. We report the preparation, purification, crys-

Table 1
Cloning details of the constructs used in this study (Dickson *et al.*, 1994).

	SCD_E321K mHsp60	mHsp10
Source organism	Human (*Homo sapiens*)	Mouse (*Mus musculus*)
Forward primer	TAA**GGATCC**CGCCAAAGATGTAAAATTT	See Viitanen *et al.* (1992)
Reverse primer	TAA**GCGGCCGC**TTAAGGGTCCTTCTCT	See Viitanen *et al.* (1992)
Expression vector	pET-21d, N-terminal His_8 tag + TEV protease site	pET-24d, C-terminal His_6 tag
Complete amino-acid sequence of the construct produced	GSAKDVKFGADARALMLQGVDLLADAVAVTMGPKGRT-VIIEQSWGSPKVTKDGVTVAKSIDLKDKYKNIGAKLV-QDVANNTNEEAGDGTTTATVLARSIAKEGFEKISKGA-NPVEIRRGVMLAVDAVIAELKKQSKPVTTPEEIAQVAT-ISANGDKEIGNIISDAMKKVGRKGVITVKDGKTLNDE-LEIIEGMKFDRGYISPYFINTSKGQKCEFQDAYVLLSEK-KISSIQSIVPALEIANAHRKPLVIIAEDVDGEALSTLVLN-RLKVGLQVVAVKAPGFGDNRKNQLKDMAIATGGAV-FGEEGLTLNLEDVQPHDLGKVGKVIVTKDDAMLLKG-KGDKAQIEKRIQEIIEQLDVTTSEYEKEKLNERLAKL-SDGVAVLKVGGTSDVEVNEKKDRVTDALNATRAAV-EEGIVLGGGCALLRCIPALDSLTPANEDQKIGIEIIKRT-LKIPAMTIAKNAGVEGSLIVEKIMQSSSEVGYDAMAG-DFVNMVEKGIIDPTKVVRTALLDAAGVASLLTTAEVV-VTEIPKEEKDP	MAGQAFRKFLPLFDRVLVERSAAETVTKGGIMLPEKSQGKV-LQATVVAVGSGGKGKSGEIEPVSVKVGDKVLLPEYGGTK-VVLDDKDYFLFRDSDILGKYVDKLAAALEHHHHHH

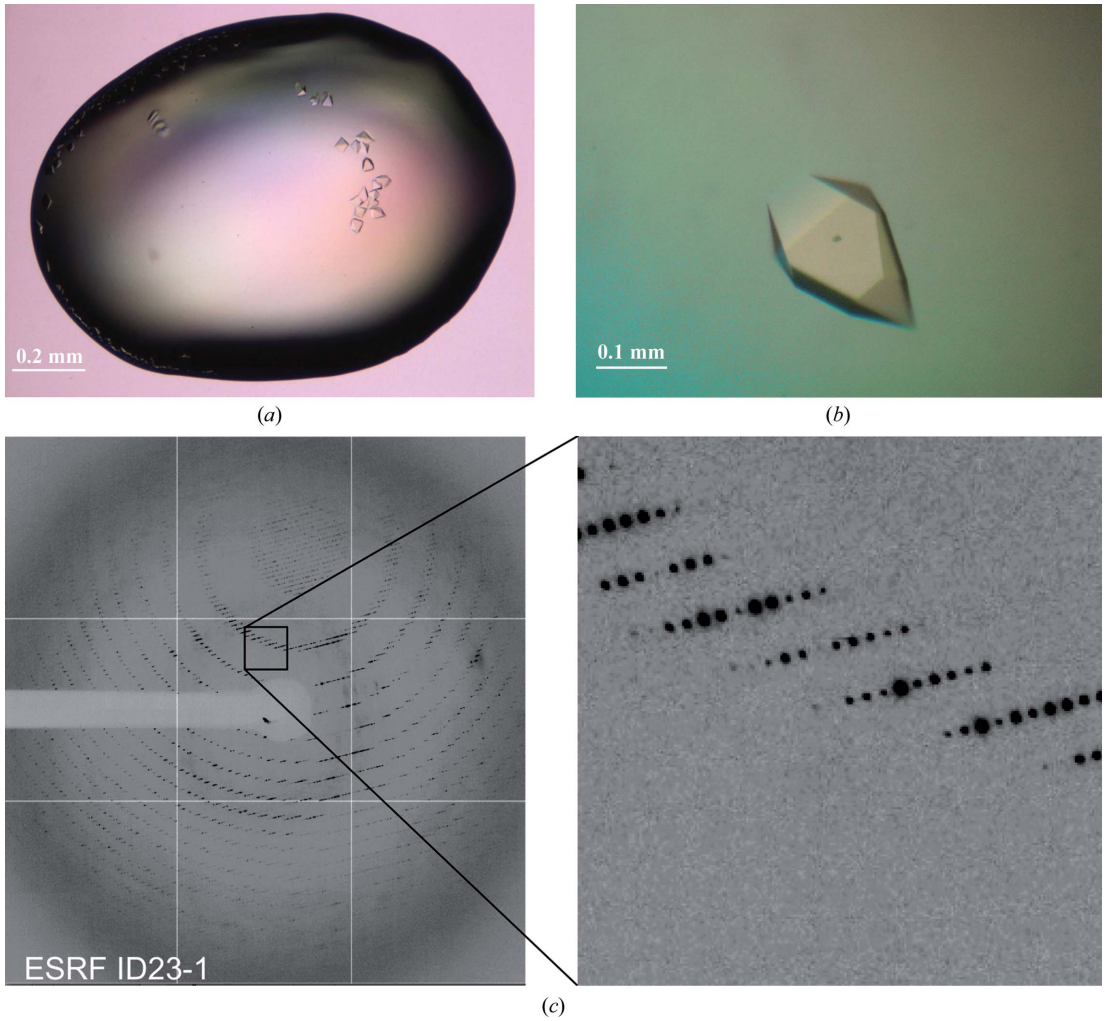

(*a*) (*b*) (*c*)

Figure 1
Crystals of the mHsp60^{E321K}–mHsp10 complex obtained from initial screening (*a*) and after optimization of the crystallization conditions (*b*). The diffraction pattern (*c*) extended to 3.5 Å resolution (at the frame edge) after dehydration. Magnification of the diffraction region shows excellent spot separation. Data were collected on beamline ID23-1 at the ESRF.

Table 2
Crystallization conditions of the crystals reported in this study.

Method	Hanging drop
Plate type	Linbro
Temperature (K)	303 for 3 d then 293
Protein concentration	mHsp60, 9.5 mg ml^{-1}; mHsp10, 1.6 mg ml^{-1}
Buffer composition of protein solution	50 m*M* Tris–HCl pH 7.7, 300 m*M* NaCl, 5% glycerol, 15 m*M* $MgCl_2$, 0.5 m*M* KCl, 1 m*M* ATP
Composition of reservoir solution	0.2 *M* ammonium acetate, 0.1 *M* sodium citrate tribasic dehydrate, 30–35%(*v*/*v*) PEG 400
Volume and ratio of drop	5 µl (1:1)
Volume of reservoir (µl)	500

tallization and structure determination by the molecular-replacement method of the mammalian mitochondrial chaperonin complex HSP60–HSP10 at a resolution of 3.34 Å. This structure shows the double-ring football-like assembly of the mHsp60–mHsp10 complex.

2. Materials and methods

2.1. Protein preparation

2.1.1. mHsp60^{E321K}. A DNA fragment encoding mHsp60, corresponding to residues 27–556 of the full-length mHsp60 (GenBank accession No. P10809), was amplified by PCR using the oligonucleotide primers listed in Table 1. The PCR product was inserted into modified pET-21d (Iosefson *et al.*, 2007) *via* *Bam*HI and *Not*I (the restriction sites in the primer sequences are shown in bold) to generate the expression plasmid. Site-directed mutagenesis (E321K mutation) was performed as described by Parnas *et al.* (2012). mHsp60^{E321K} was expressed and purified as described by Parnas *et al.* (2009).

The purified protein solution consisted of ∼30 mg ml^{-1} protein, 50 m*M* Tris–HCl pH 7.7, 300 m*M* NaCl, 5% glycerol and 10 m*M* $MgCl_2$.

2.1.2. mHsp10. mHsp10 was cloned and purified as described by Dickson *et al.* (1994) and Parnas *et al.* (2009) (Table 1). The purified protein solution consisted of ∼30 mg ml^{-1} protein, 50 m*M* Tris–HCl pH 7.7 and 100 m*M* NaCl.

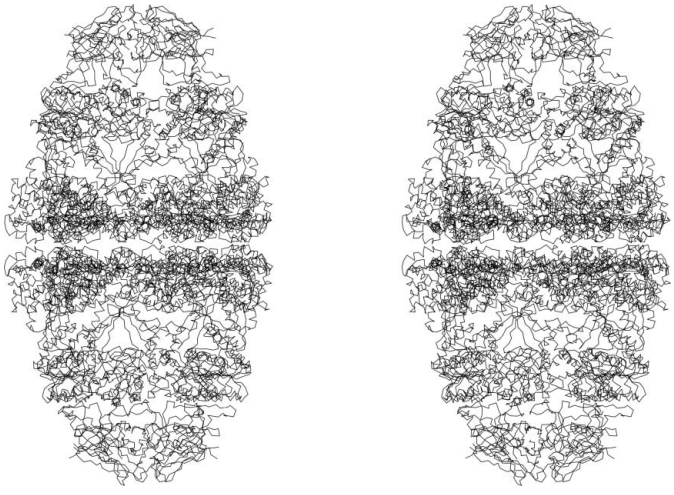

Figure 2
Wall-eyed stereoview of the C$^{\alpha}$ trace of the structure of the mHsp60^{E321K}–mHsp10 complex.

Table 3
Data collection and processing.

Values in parentheses are for the highest resolution shell.

Diffraction source	ID23-1, ESRF
Wavelength (Å)	0.95370
Temperature (K)	100
Detector	ADSC Q15
Crystal-to-detector distance (mm)	550.7
Rotation range per image (°)	0.5
Total rotation range (°)	100
Exposure time per image (s)	0.3
Space group	$P4_12_12$
Unit-cell parameters (Å)	$a = b = 198.11$, $c = 625.04$
Mosaicity range (°)	0.18–0.45
Resolution range (Å)	30–3.34 (3.40–3.34)
Total No. of reflections	1440760 (58205)
No. of unique reflections	179444 (8831)
Completeness (%)	100.0 (100.0)
Multiplicity	8.1 (6.6)
$\langle I/\sigma(I)\rangle$	12.1 (1.2)†
$CC_{1/2}$ for the highest resolution shell	0.527
$R_{r.i.m.}$‡	0.066 (0.584)
Overall *B* factor from Wilson plot (Å^2)	81.1§

† The resolution cutoff decision was made using the approach of Karplus & Diederichs (2012). $\langle I/\sigma(I)\rangle$ falls below 2.0 at 3.46 Å resolution. The data were collected before the paper describing the $CC_{1/2}$ approach was published. ‡ Calculated by multiplying the conventional R_{merge} value by the factor $[N/(N-1)]^{1/2}$, where N is the multiplicity. § The Wilson plot does not show anomalies.

2.2. Crystallization

mHsp60 and mHsp10 were mixed together with 1 m*M* ATP and incubated for 5 min at 293 K immediately before setting up crystallization drops. Preliminary screening of crystallization conditions was performed using the hanging-drop vapour-diffusion method with the PEGRx 1, PEGRx 2, Index, Natrix, PEG/Ion (Hampton Research) and The JCSG+ Suite (Qiagen) crystallization kits at the Israel Structural Proteomics Center, Weizmann Institute of Science, Rehovot, Israel using a Mosquito crystallization robot (TTP LabTech, Royston, England) at 293 K. Crystals of the mHsp60–mHsp10 complex were observed after 1 d (Fig. 1*a*). Crystallization conditions were optimized in standard 24-well Linbro plates (Hampton Research) (Fig. 1*b*, Table 2). These crystals yielded diffraction to 7–8 Å resolution. The diffraction quality was significantly improved by dehydration with PEG 400 (Fig. 1*c*). In this process, after crystal growth, the cover slips were transferred to reservoirs containing serially increasing PEG 400 concentrations in the mother liquor. The concentration of PEG 400 was increased by 15% in three consecutive steps of 5% with ∼24 h incubation time for each step (35, 40 and 45%). All dehydration procedures were carried out at a temperature of 293 K.

2.3. Data collection and processing

The dehydrated crystals were harvested from hanging drops using cryo-loops, oriented along the longest axis, plunged into liquid nitrogen and placed in pucks for transportation to the synchrotron at cryogenic temperature. Crystals were mounted in the diffraction position utilizing the standard sample changer at the European Synchrotron Radiation Facility (ESRF), Grenoble, France. Diffraction data were collected, integrated and scaled using *DENZO* and *SCALEPACK* as implemented in *HKL*-2000 (Otwinowski & Minor, 1997). Diffraction data statistics are shown in Table 3.

2.4. Crystal structure determination

By implementing the molecular-replacement method, the structure of the complex was successfully determined using as a model the GroEL seven-member upper extended ring (*cis* ring) together with

its bound GroES seven-membered lid (with 48.6% identity to the sequence of the mammalian mitochondrial chaperonin and 32.7% identity to that of the co-chaperonin) derived from PDB entry 1aon (Xu *et al.*, 1997). The molecular-replacement program *MOLREP* (v.11.1.03; Vagin & Teplyakov, 2010) was used as implemented in the *CCP*4 suite (v.6.3.0; Winn *et al.*, 2011). Solute molecules and ATP/ADP cofactors were deleted from the model coordinate file. The model coordinates were not trimmed to the unequivocal structure. The molecular-replacement solution (score 0.233, translation-function peak/noise 17.92 and contrast 12.38) revealed that 14 mHsp60 and 14 mHsp10 molecules were arranged in an elliptical 'football'-like assembly.

Refinement of the structure started at $R_{\rm model}$ = 0.5169 and $R_{\rm free}$ = 0.5164 and reached $R_{\rm model}$ = 0.3595 and $R_{\rm free}$ = 0.4176 after 100 cycles of refinement using *REFMAC* (v.5.7.32; Murshudov *et al.*, 2011) with activated jelly-body option, the use of secondary-structure restraints as generated by *ProSMART* (v.0.816; Nicholls *et al.*, 2012) and the application of NCS torsion-angle restraints, unequivocally supporting the correctness of the molecular-replacement solution. The GroEL–GroES sequence was still preserved after the initial refinement. Fig. 2 presents the C^{α} trace of the determined structure in cross-eyed stereo. Refinement and rebuilding of the structure are currently under way in our laboratory.

3. Conclusion

We report the first X-ray structural determination of the mammalian mitochondrial Hsp60–Hsp10 complex. The structure revealed a symmetrical 'football'-shaped complex of the chaperonin in complex with the co-chaperonin. The formation of symmetrical complexes was demonstrated for the first time for GroEL–GroES complexes from *E. coli* using a variety of low-resolution methods (Azem *et al.*, 1994; Schmidt *et al.*, 1994; Todd *et al.*, 1994; Harris *et al.*, 1994; Llorca *et al.*, 1994). To the best of our knowledge, however, no high-resolution X-ray structure has been published to date for a symmetrical complex of chaperonins.

We thank the ESRF, Grenoble, France for use of the macromolecular crystallographic data-collection facilities and the ID23-1 staff for their assistance. This work was supported by a grant from the Morasha program of the Israel Science Foundation (Grant 1902/08) and Israel Science Foundation Grant 452/09 (to AA) and by an Eshkol Fellowship from the Ministry of Science (to SN)

References

Azem, A., Kessel, M. & Goloubinoff, P. (1994). *Science*, **265**, 653–656.
Braig, K., Otwinowski, Z., Hegde, R., Boisvert, D. C., Joachimiak, A., Horwich, A. L. & Sigler, P. B. (1994). *Nature (London)*, **371**, 578–586.
Bross, P., Magnoni, R. & Bie, A. S. (2012). *Curr. Top. Med. Chem.* **12**, 2491–2503.
Cappello, F., Conway de Macario, E., Marasà, L., Zummo, G. & Macario, A. J. (2008). *Cancer Biol. Ther.* **7**, 801–809.
Cheng, M. Y., Hartl, F.-U., Martin, J., Pollock, R. A., Kalousek, F., Neupert, W., Hallberg, E. M., Hallberg, R. L. & Horwich, A. L. (1989). *Nature (London)*, **337**, 620–625.
Czarnecka, A. M., Campanella, C., Zummo, G. & Cappello, F. (2006). *Cancer Biol. Ther.* **5**, 714–720.
Deocaris, C. C., Kaul, S. C. & Wadhwa, R. (2006). *Cell Stress Chaperones*, **11**, 116–128.
Dickson, R., Larsen, B., Viitanen, P. V., Tormey, M. B., Geske, J., Strange, R. & Bemis, L. T. (1994). *J. Biol. Chem.* **269**, 26858–26864.
Ellis, R. J. (2003). *Curr. Biol.* **13**, R881–R883.
Gupta, S. & Knowlton, A. A. (2005). *J. Cell. Mol. Med.* **9**, 51–58.
Harris, J. R., Plückthun, A. & Zahn, R. (1994). *J. Struct. Biol.* **112**, 216–230.
Hunt, J. F., Weaver, A. J., Landry, S. J., Gierasch, L. & Deisenhofer, J. (1996). *Nature (London)*, **379**, 37–45.
Iosefson, O., Levy, R., Marom, M., Slutsky-Leiderman, O. & Azem, A. (2007). *Protein Sci.* **16**, 316–322.
Karplus, P. A. & Diederichs, K. (2012). *Science*, **336**, 1030–1033.
Levy-Rimler, G., Bell, R. E., Ben-Tal, N. & Azem, A. (2002). *FEBS Lett.* **529**, 1–5.
Llorca, O., Marco, S., Carrascosa, J. L. & Valpuesta, J. M. (1994). *FEBS Lett.* **345**, 181–186.
Murshudov, G. N., Skubák, P., Lebedev, A. A., Pannu, N. S., Steiner, R. A., Nicholls, R. A., Winn, M. D., Long, F. & Vagin, A. A. (2011). *Acta Cryst.* D**67**, 355–367.
Nicholls, R. A., Long, F. & Murshudov, G. N. (2012). *Acta Cryst.* D**68**, 404–417.
Nielsen, K. L. & Cowan, N. J. (1998). *Mol. Cell*, **2**, 93–99.
Nielsen, K. L., McLennan, N., Masters, M. & Cowan, N. J. (1999). *J. Bacteriol.* **181**, 5871–5875.
Osterloh, A., Meier-Stiegen, F., Veit, A., Fleischer, B., von Bonin, A. & Breloer, M. (2004). *J. Biol. Chem.* **279**, 47906–47911.
Ostermann, J., Horwich, A. L., Neupert, W. & Hartl, F.-U. (1989). *Nature (London)*, **341**, 125–130.
Otwinowski, Z. & Minor, W. (1997). *Methods Enzymol.* **276**, 307–326.
Parnas, A., Nadler, M., Nisemblat, S., Horovitz, A., Mandel, H. & Azem, A. (2009). *J. Biol. Chem.* **284**, 28198–28203.
Parnas, A., Nisemblat, S., Weiss, C., Levy-Rimler, G., Pri-Or, A., Zor, T., Lund, P. A., Bross, P. & Azem, A. (2012). *PLoS One*, **7**, e50318.
Samali, A., Cai, J., Zhivotovsky, B., Jones, D. P. & Orrenius, S. (1999). *EMBO J.* **18**, 2040–2048.
Schmidt, M., Rutkat, K., Rachel, R., Pfeifer, G., Jaenicke, R., Viitanen, P., Lorimer, G. & Buchner, J. (1994). *Science*, **265**, 656–659.
Todd, M. J., Viitanen, P. V. & Lorimer, G. H. (1994). *Science*, **265**, 659–666.
Vagin, A. & Teplyakov, A. (2010). *Acta Cryst.* D**66**, 22–25.
Viitanen, P. V., Gatenby, A. A. & Lorimer, G. H. (1992). *Protein Sci.* **1**, 363–369.
Winn, M. D. *et al.* (2011). *Acta Cryst.* D**67**, 235–242.
Xu, Z., Horwich, A. L. & Sigler, P. B. (1997). *Nature (London)*, **388**, 741–750.